

The Essential Role of Hippocampal CA1 NMDA Receptor–Dependent Synaptic Plasticity in Spatial Memory

Joe Z. Tsien, Patricio T. Huerta,
and Susumu Tonegawa
Howard Hughes Medical Institute
Center for Learning and Memory
Center for Cancer Research
Department of Biology
Massachusetts Institute of Technology
Cambridge, Massachusetts 02139

Summary

We have produced a mouse strain in which the deletion of the *NMDAR1* gene is restricted to the CA1 pyramidal cells of the hippocampus by using a new and general method that allows CA1-restricted gene knockout. The mutant mice grow into adulthood without obvious abnormalities. Adult mice lack NMDA receptor-mediated synaptic currents and long-term potentiation in the CA1 synapses and exhibit impaired spatial memory but unimpaired nonspatial learning. Our results strongly suggest that activity-dependent modifications of CA1 synapses, mediated by NMDA receptors, play an essential role in the acquisition of spatial memories.

Introduction

It has long been hypothesized that memory storage in the mammalian brain involves modifications of the synaptic connections between neurons. Hebb (1949) introduced an influential theory consisting of principles that neurons must exhibit for implementing associative memory. An important principle, known as the Hebb rule, is that of “correlated activity”: when the presynaptic and the postsynaptic neurons are active simultaneously, their connections become strengthened. It is well established that *N*-methyl-D-aspartate receptors (NMDARs) can implement the Hebb rule at the synaptic level, and they are thus considered the crucial synaptic elements for the induction of activity-dependent synaptic plasticity. NMDARs act as coincidence detectors because they require both presynaptic activity (glutamate released by axonal terminals) and postsynaptic activity (depolarization that releases the Mg²⁺ block) as a condition for channel opening (Nowak et al., 1984; McBain and Mayer, 1994). Active NMDAR channels allow calcium influx into the postsynaptic cell, which triggers a cascade of biochemical events resulting in synaptic change. Long-term potentiation (LTP) is a widely used paradigm for increasing synaptic efficacy, and its induction requires, in at least one of its forms, the activation of NMDARs (Bliss and Lømo, 1973; Bliss and Collingridge, 1993). Conventionally, NMDAR-dependent LTP is elicited by giving a strong pattern of electrical stimulation (a 25–100 Hz train for ~1 s) to the inputs, which triggers a rapid and lasting increase in synaptic strength.

The hippocampus is the most intensely studied region for the importance of NMDARs in synaptic plasticity and

memory. It is well known that lesions of the hippocampus in humans and other mammals produce severe amnesia for certain memories (Scoville and Milner, 1957; Morris et al., 1982; Zola-Morgan et al., 1986; reviewed by Squire, 1987). Importantly, it has been demonstrated that disruption of NMDARs in the hippocampus leads to blockade of synaptic plasticity and also to memory malfunction (reviewed by Morris et al., 1991; Rawlins, 1996). For instance, application of NMDAR antagonists (such as 2-amino-5-phosphonopropionic acid [AP5]) completely blocks the induction of LTP in most hippocampal synapses (Collingridge et al., 1983; Zalutsky and Nicoll, 1990; Hanse and Gustafsson, 1992). Morris et al. (1986) were the first to show that rats that received infusion of AP5 into the hippocampus were deficient in performing a spatial memory task in which the animals are required to form multiple spatial relations between a hidden platform in a circular pool (known as a water maze) and visible objects in the surrounding environment and swim to the platform to escape from the water. Subsequently, this issue was reinvestigated by using “gene knockout” mice. These genetically engineered mice lack a gene encoding a component that is thought to be at the downstream of activated NMDARs in the biochemical cascade for LTP induction (reviewed by Chen and Tonegawa, 1997). For example, mice with a deletion in the gene encoding the α subunit of calcium-calmodulin-dependent protein kinase II (α CaMKII) display impaired LTP in the CA1 region of the hippocampus and a deficit in spatial learning (Silva et al., 1992a, 1992b).

Even though the results of these genetic and pharmacological experiments are consistent with the notion that hippocampal LTP is the synaptic mechanism for spatial memory, other interpretations cannot be excluded. For instance, in the case of the gene knockout mice, every cell in the organism lacks the gene of interest. Consequently, all of the functions of the gene product, not only its role in LTP induction, are affected in the mutants. Hence, it is possible that spatial memory is independent of hippocampal LTP and that the memory deficit in mutants arises from lack of the gene product in other functions (such as developmental roles). Likewise, in pharmacological studies the target of the AP5 infusion is not restricted to the hippocampus (Butcher et al., 1991). Therefore, NMDARs expressed in neurons in the neighboring neocortex (and other brain areas) are also inhibited to a varying extent. Since NMDARs contribute substantially to the basal synaptic transmission of excitatory synapses in the neocortex (reviewed by Hestrin, 1996), it is likely that the infused AP5 may impair not only LTP induction in the hippocampus but also the computational ability of neocortical regions that play an important role in spatial memory.

A way to circumvent the aforementioned problems is to modify the gene knockout method such that the deletion is restricted to a certain region or a certain cell type within the brain. As described in the accompanying article (Tsien et al., 1996 [this issue of *Cell*]), we have exploited the *Cre/loxP* recombination system derived

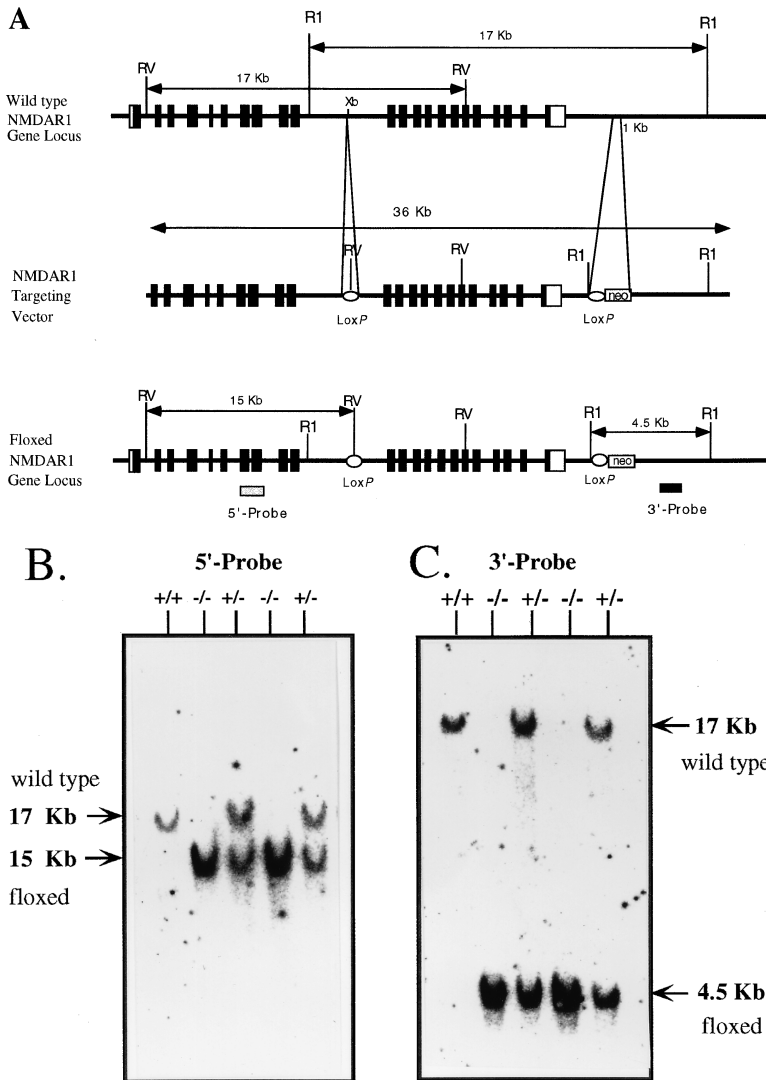


Figure 1. Targeted Disruption of the *NMDAR1* Subunit Gene

(A) The *NMDAR1* locus and targeting construct. (Top) The wt genomic region that contains the *NMDAR1* gene. (Middle) The *NMDAR1* targeting vector that contains two *loxP* sequences. (Bottom) The floxed *NMDAR1* gene.

(B and C) Southern blot analysis of representative tail biopsies. Tail DNA was digested with *EcoRV* for blotting with a 5' probe and with *EcoRI* for blotting with a 3' probe. The size of the expected band is indicated. +/+, wild type; +/-, heterozygous; -/-, homozygous fNR1 mutants.

from the phage P1 and have developed a method that can potentially restrict the deletion of any gene of interest to the pyramidal cells of the hippocampal CA1 region. Here we describe an application of this method to the *NMDA receptor 1* gene (*NMDAR1*), which encodes the essential subunit for the NMDAR (Moriyoshi et al., 1991; Nakanishi, 1992). We demonstrate that the *NMDAR1* gene is deleted exclusively in the CA1 pyramidal cells in the mutant mice ("NMDAR1 CA1-KO" mice or simply "CA1-KO" mice). These mice grow into adulthood without obvious pathologies, in contrast to the *NMDAR1* KO mice produced by conventional gene targeting that die neonatally (Li et al., 1994, Forrest et al., 1994). We report that the CA1-KO mice lack NMDAR-mediated postsynaptic currents and LTP in the CA1 region. Also, these mice show impaired spatial memory (measured in the hidden-platform version of the Morris water maze) but display good performance in nonspatial learning tasks. These results provide strong support for the hypothesis that NMDAR-mediated LTP in the CA1 region is crucially involved in the formation of certain types of memory.

Results

Generation of CA1-Restricted *NMDAR1* Mutant Mice

We constructed a targeting vector in which two *loxP* sequences were inserted into the *NMDAR1* gene. The first *loxP* sequence was placed in the intron that lies between exons 10 and 11, whereas the second *loxP* sequence and a neomycin-resistance gene were introduced in the downstream region of the 3' end of the *NMDAR1* gene (Figure 1A). In this manner, the two *loxP* sequences flank a region of the *NMDAR1* gene that encodes the four transmembrane domains as well as the entire C-terminal sequence of the polypeptide chain. Embryonic stem (ES) cells were transfected with the linearized targeting vector and were tested for homologous recombination by Southern blot. The targeted ES cells were then injected into blastocysts, and mice homozygous for the *loxP-NMDAR1-loxP* sequence (henceforth named "floxed NR1" or simply "fNR1," where floxed stands for "flanked by *loxP*") were generated (Fig-

ures 1B and 1C) through standard procedures (Bradley, 1987; Capecchi, 1989).

We crossed *fNR1* mice with heterozygous *Cre* transgenic mice, T29-1, which have the capacity to mediate *Cre/loxP* recombination exclusively in the CA1 pyramidal cells (Tsien et al., 1996). After crossing, we obtained mice carrying the *Cre* transgene and the homozygous *fNR1* gene (*Cre/+*, *fNR1/fNR1*)—that is, CA1-KO mice—as well as various types of siblings (see Experimental Procedures). From the latter, wild-type (wt) mice (+/+), T29-1 mice (*Cre/+*, +/+), and homozygous *fNR1* mice (+/+, *fNR1/fNR1*) were used as experimental controls. The proportions of mice of the various genotypes indicated, first, that *Cre* and *fNR1* segregate as independent Mendelian loci, and second, that the CA1-KO mice and the homozygous *fNR1* mice are not lethal at the embryonic or perinatal stages. Indeed, these two types of mice grow and mate normally, and their overall behavior is indistinguishable from that of wt and T29-1 mice. These characteristics of the CA1-KO and the homozygous *fNR1* mice are in contrast to the perinatal lethality of NMDAR1 KO mice produced by conventional gene knockout (Li et al., 1994; Forrest et al., 1994). The absence of a gross behavioral phenotype suggests both that the *loxP* insertions do not interfere with normal expression of the *fNR1* gene and that the *NMDAR1* deletion in CA1-KO mice must be regionally restricted, as expected.

Histochemical examination showed that the brains from the CA1-KO mice did not exhibit any obvious abnormalities at the macroscopic level (Figure 2). In addition, we examined the neuronal patterns of the “whisker-to-barrels” system representing the mouse whiskers. The formation of these patterns has been reported to be dependent on NMDAR function at the level of the trigeminal brainstem nucleus (Li et al., 1994). We found that the mutant mice exhibited well-formed patterns in the brainstem trigeminal nucleus (Figure 2G), the ventrobasal nucleus of the thalamus (Figure 2H), and the primary somatosensory neocortex (Figure 2I). Furthermore, we confirmed the CA1-restricted deletion of the *NMDAR1* gene in the CA1-KO mice by *in situ* hybridization with a probe whose sequence should be deleted at the DNA level by the *Cre/loxP* recombination. The CA1 region of the mutant mice appeared to lack expression of *NMDAR1* mRNA (Figure 3), whereas expression in other brain regions (such as CA3, dentate gyrus, and neocortex) was indistinguishable from control mice (Figure 3).

Synaptic Transmission in CA1 and Dentate Gyrus

Synaptic responses of CA1 pyramidal neurons were evoked by stimulation of Schaffer collateral/commissural (Scc) afferents in acute slices. Whole-cell recordings revealed that the CA1-KO cells lacked the slow component of the excitatory postsynaptic current (EPSC) that is mediated by NMDARs (Hestrin et al., 1990a, 1990b). Conversely, the early component of the EPSC that is mediated by α -amino-3-hydroxy-5-methyl-4-isoxazolepropionate (AMPA) receptors was intact in the mutants (Figure 4A). Blockade of AMPA receptors with

6-cyano-7-dinitroquinoxaline-2,3-dione (CNQX) (20 μ M) resulted in a complete inhibition of the EPSC in the mutant cells, whereas the control cells displayed a robust isolated NMDAR-dependent EPSC (Figure 4A). Furthermore, the current-voltage relations for the AMPA and NMDA components of the EPSC showed that the AMPA currents were not different between mutant and control cells, but the NMDA component was absent in the CA1-KO cells (Figure 4B). The reversal potential for the early component of the EPSC in mutants (2 ± 1 mV, $n = 8$) was similar to that in the control cells (T29-1, 3 ± 2 mV, $n = 5$; *fNR1*, 2 ± 2 mV, $n = 4$).

We used field recordings of excitatory postsynaptic potentials (EPSPs) to examine further the synaptic properties of mutant slices. The time courses of the EPSPs measured in CA1 were similar between mutant slices (Figure 5A, left) and control slices (data not shown), when they were bathed with standard saline solution. However, addition of a solution that isolates the NMDARs (see Experimental Procedures) resulted in complete blockade of the EPSPs in mutant slices ($n = 12$; Figure 5A, left). Conversely, the control slices showed a distinct isolated NMDA EPSP in CA1 (data not shown).

A key control experiment was to examine whether functional NMDARs are present in other brain structures in the CA1-KO mice. We studied the synaptic responses of granule cells in the dentate gyrus upon stimulation of the lateral perforant path (Hanse and Gustafsson, 1992). We found that the time courses of field EPSPs in mutant slices (Figure 5A, right) looked normal when compared with control slices (data not shown). Importantly, after addition of a solution that isolates NMDARs, the mutant slices showed clear NMDA EPSPs ($n = 12$; Figure 5A, right) as well as the control slices (data not shown).

In addition, we computed the input-output relations of the field EPSPs in CA1, a relation that is used as a measure of the efficiency of synaptic transmission. The input is given by the amplitude of the fiber volley (presynaptic action potential) that precedes the postsynaptic response, whereas the output is given by the initial slope of the EPSP. The input-output relations were indistinguishable between the CA1-KO and control slices (Figure 5B). Moreover, the paradigm of paired pulse facilitation, which gives an indication of presynaptic function, showed no differences between the mutant and control slices (Figure 5C).

In conclusion, our electrophysiological analysis reveals that the CA1-KO mice lack functional postsynaptic NMDARs in the CA1 pyramidal cells. By contrast, postsynaptic AMPA receptors as well as presynaptic terminals seem to operate normally in CA1. Finally, the CA1-KO mice show normal NMDAR function in the dentate gyrus.

Synaptic Plasticity in CA1 and Dentate Gyrus

Scc inputs onto CA1 neurons were stimulated at 0.1 Hz with single shocks, each of which evoked a single field EPSP (Huerta and Lisman, 1995). Application of tetanic stimulation (100 Hz for 1 s) failed to induce LTP in the

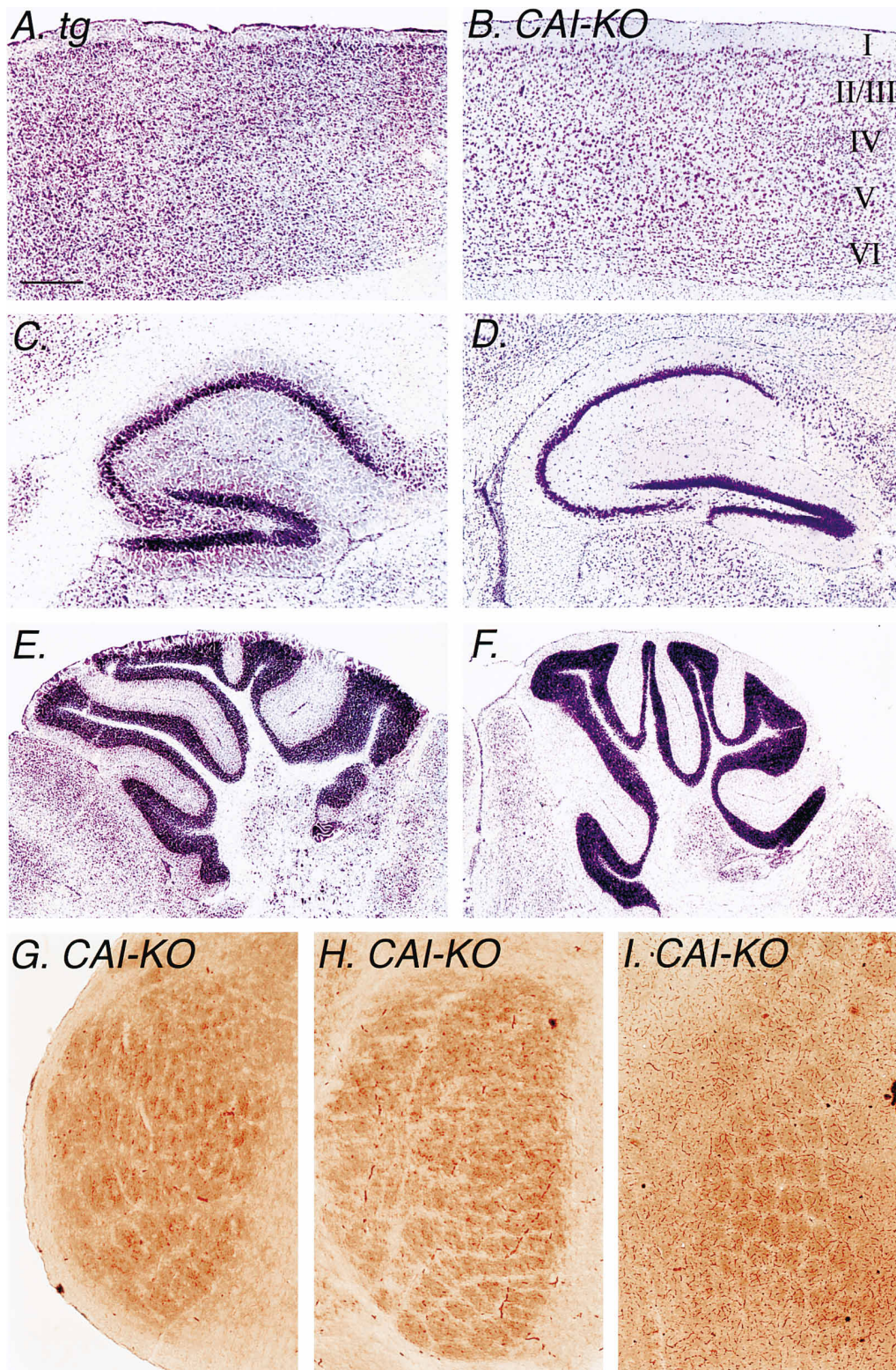


Figure 2. Morphology of the Control (T29-1) and CA1-KO Brains

(A and B) Nissl stains of sagittal sections through the neocortex of T29-1 and CA1-KO mice. The cortical layers are indicated by the numbers. Scale bar, 200 μ m.

(C and D) Nissl stains of sagittal sections through the hippocampus of T29-1 and CA1-KO mice.

(E and F) Nissl stains of sagittal sections through the cerebellum of T29-1 and CA1-KO mice.

(G-I) Cytochrome oxidase-stained sections in CA1-KO mice. (G) Barrelettes in the brainstem trigeminal nucleus (P8 mouse), (H) barreloids in the thalamus (P8 mouse), and (I) barrels in the primary somatosensory neocortex (adult mouse).

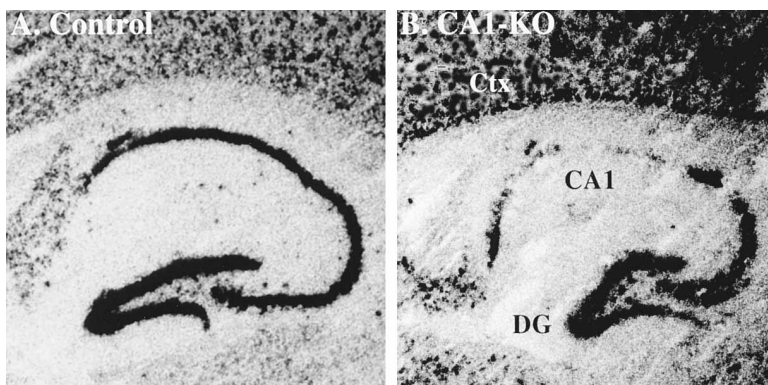


Figure 3. Lack of the NMDAR1 Subunit in the CA1 Region

In situ hybridization of *NMDAR1* mRNA from wt (A) and CA1-KO (B) brains. ctx, cortex; DG, dentate gyrus.

CA1-KO slices (Figure 6A). Moreover, short-term potentiation was not detectable in the mutant slices. On average, the synaptic responses were unchanged in CA1-KO slices 45 min after the tetanus ($100.4 \pm 4.9\%$, $n = 21$; Figure 6B), whereas LTP was readily obtained in control slices (T29-1, $168.5 \pm 4.9\%$, $n = 12$; fNR1, $156.9 \pm 8.3\%$, $n = 4$; wt, $177.7 \pm 6.2\%$, $n = 5$; Figure 6B). Comparison of the “tetanized” pathway with the “nontetanized” pathway (i.e., pathways 1 and 2, respectively, in Figure 6A, right) in each control group revealed that the enhancement was statistically significant ($p < 0.005$ for each group, *t* test).

Furthermore, we attempted to induce NMDAR-dependent long-term depression (LTD) in CA1-KO slices by giving a low frequency train of 1 Hz for 10 min (Dudek and Bear, 1992). This stimulation was unable to produce LTD ($94.8 \pm 12.6\%$, 45 min after train, $n = 4$, not shown). By contrast, we were able to elicit NMDAR-independent LTP in mutant slices by giving a very high frequency tetanus (four trains, each train 250 Hz for 0.2 s, 5 s between trains). This paradigm induced a slowly rising synaptic increase ($35.2 \pm 8.4\%$, 60 min after tetanus,

$n = 4$, $p < 0.01$, *t* test, data not shown), demonstrating the preservation of an NMDAR-independent LTP mechanism in the CA1 region (Grover and Teyler, 1990).

Finally, we examined whether LTP could be induced in the mutant dentate gyrus. Lateral perforant path and medial perforant path inputs onto granule cells were stimulated at 0.1 Hz (Hanse and Gustafsson, 1992). Tetanic stimulation (40 shocks at 100 Hz) was able to induce LTP in either of the two inputs (Figure 6C). On average, the lateral perforant path showed a statistically significant increase in synaptic efficacy 45 min after the tetanus ($154.6 \pm 10.1\%$, $n = 10$, $p < 0.01$, *t* test; Figure 6D). In a few experiments, we confirmed that this LTP is NMDAR-dependent because addition of AP5 ($50 \mu\text{M}$) completely blocked its induction ($99.1 \pm 3.1\%$, $n = 3$, data not shown).

Spatial Memory

To test for spatial memory we trained mice in a water maze to find a fixed, hidden platform by using distal cues (Morris et al., 1982; Huerta et al., 1996). We found that the CA1-KO mice were deficient in learning this task

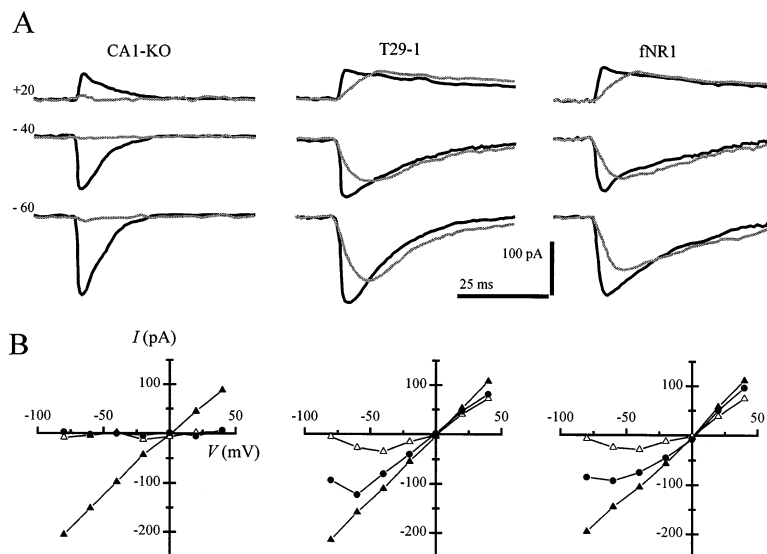


Figure 4. NMDAR1 CA1-KO Pyramidal Neurons Lack Functional NMDARs in the CA1 Region

(A) Representative traces of EPSCs recorded from CA1-KO (left), T29-1 (middle), and fNR1 (right) cells in the whole-cell voltage clamp mode (numbers at left are the holding potentials; each trace is the average of 20 consecutive responses). The solid traces correspond to dual-component EPSCs recorded in standard saline solution (which contains $1.3 \mu\text{M}$ Mg^{2+}), and the shaded traces correspond to the isolated NMDA receptor-mediated EPSCs recorded in a solution containing CNQX ($20 \mu\text{M}$), 2-OH-saclofen ($200 \mu\text{M}$), and glycine ($1 \mu\text{M}$) and nominally Mg^{2+} free. It is clear that the CA1-KO neuron (left) lacks the slow component of the EPSC and the isolated NMDA EPSC.

(B) Current to voltage relations for representative CA1-KO (left), T29-1 (middle), and fNR1 (right) cells. In standard saline, the fast component (closed triangles, measured as the peak amplitude of the EPSC) looks similar

in the three cases, but the slow component (open triangles, measured as the average amplitude 25–30 ms after the onset of the EPSC) is disrupted in the CA1-KO cell. A similar result is observed for the isolated NMDA EPSC (closed circles, measured as the peak amplitude), which is normal in the T29-1 and fNR1 cells but absent in the CA1-KO mutant cells.

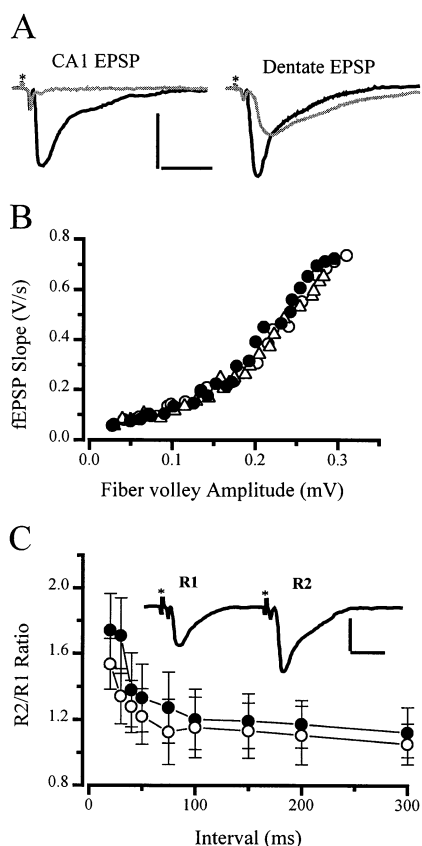


Figure 5. Synaptic Parameters in the CA1-KO Slices

(A) Representative traces (average of 10 responses) of field EPSPs measured in the stratum radiatum of the CA1 region (left) and in the stratum moleculare of the dentate gyrus (right) in CA1-KO slices. The solid traces correspond to EPSPs measured in standard saline, while the shaded traces correspond to EPSPs measured in a solution containing CNQX (20 μ M), 2-OH-saclofen (200 μ M), and glycine (1 μ M), and nominally Mg^{2+} free. The isolated NMDA EPSP is absent in CA1 (left) and clearly distinguishable in dentate (right). Scale, 0.5 mV, 10 ms.

(B) Input-output relations measured in CA1 appear normal in the mutants. The CA1-KO synapses (closed circles) show a similar behavior than the control groups, T29-1 (open circles) and fNR1 (open triangles).

(C) Paired pulse facilitation appears normal in the mutants. (Inset) A representative trace (average of 5 responses) from mutant CA1 synapses in which two consecutive EPSPs were elicited with a 30 ms interval; scale, 0.5 mV, 10 ms. The second EPSP (R2) is clearly larger than the first EPSP (R1) demonstrating facilitation. The graph is the averaged ratio R2/R1 (mean \pm SEM) as a function of the interstimulus interval for mutant (closed circles) and T29-1 (open circles) slices ($n = 10$ for each group).

when compared to control siblings. Mutants consistently showed a longer escape latency over training blocks, although they displayed a progressive improvement in their escape behavior (Figure 7A). On average, CA1-KO mice took 50.3 ± 2.7 s to find the platform on the first block; that latency was reduced to 28.2 ± 3.0 s after 12 blocks. One-way analysis of variance (ANOVA) showed this reduction to be significant ($n = 43$, $F[1, 84] = 29.75$, $p < 0.0001$). The control mice also showed a significant decrease in their latencies from block 1 to block 12 ($p < 0.0001$ for each group, ANOVA). Moreover,

there was a significant effect of genotype; CA1-KO mice had significantly higher escape latencies than the control mice on all blocks ($n = 12$, $F[1, 46] = 6.64$, $p < 0.001$, ANOVA).

Even though the mutant mice showed an improvement in their escape latencies, they could be relying on nonspatial strategies to find the hidden platform. Thus, we used a "transfer" test (TT) to determine whether the mice had formed a spatial memory of the task. During this test the platform is absent and the mice swim for 60 s in the pool. If the animals use a spatial strategy (i.e., they map the position of the hidden platform by using the relations among the distal visual cues around the pool), it is expected that they spend a significantly greater amount of time than accounted for by chance actively searching for the platform in the location where they were trained to find it. By contrast, if the mice use nonspatial strategies they should spend approximately an equal amount of time in each quadrant of the pool. This could occur, for instance, if the mice learned that the platform is at a certain distance from the edge of the pool.

We gave three tests: TT1 was after block 1; TT2 was at the end of block 6; and TT3 was after block 12 (Bannerman et al., 1995). We found that in TT1 the mutants swam at chance level in each of the four quadrants of the pool and remained to do the same in TT2 and TT3 (Figures 8A and 8B). Thus, the CA1-KO mice did not show any place preference for the target quadrant in any of the TTs. In contrast, the control groups started at chance level in TT1 but showed a marked preference for the target quadrant in TT2 and remained at this same level of quadrant preference in TT3 (TT2: T29-1, 22.6 ± 2.7 s; fNR1, 27.6 ± 1.5 s; wt, 20.2 ± 2.4 s; TT3: T29-1, 21.4 ± 2.2 s; fNR1, 23.6 ± 1.9 s; wt, 26.5 ± 2.2 s; $p < 0.0001$ for all of the values, paired t test; Figure 8A). Analysis of the navigational strategies of mice during TT3 demonstrated that the control mice focused their search in the trained area and thus produced a high total occupancy peak in the position in which the platform was previously located (Figure 8C, top), whereas the mutants navigated all over the area of the pool (Figure 8C, bottom). An additional measure of spatial memory is given by the "crossings," the number of times the mice cross the correct location of the platform. On average, during TT3 the CA1-KO mutants had 1.64 ± 0.6 crossings, significantly fewer than control mice (T29-1, 4.0 ± 0.5 ; fNR1, 2.8 ± 0.5 ; wt, 4.2 ± 0.6). Also, the mutants showed a significant deficit on the "platform search," the average time searching in the exact location of the platform (CA1-KO, 0.6 ± 0.2 s; T29-1, 1.4 ± 0.3 s; fNR1, 1.0 ± 0.2 s; wt, 1.7 ± 0.3 s). Finally, to ensure that our apparatus was well suited for measuring spatial memory, we tested homozygous α CaMKII knockout mice. These mice are known to be deficient in spatial memory (Silva et al., 1992a) and indeed showed, in our apparatus, the same complete deficit in spatial memory as the CA1-KO mice (data not shown).

To assess whether the impaired behavior of the mutants in the hidden-platform version of the water maze was not due to some sensorimotor or motivational deficit, we trained the mice in a simpler task in the water maze (Kolb et al., 1994). In this task the animals are

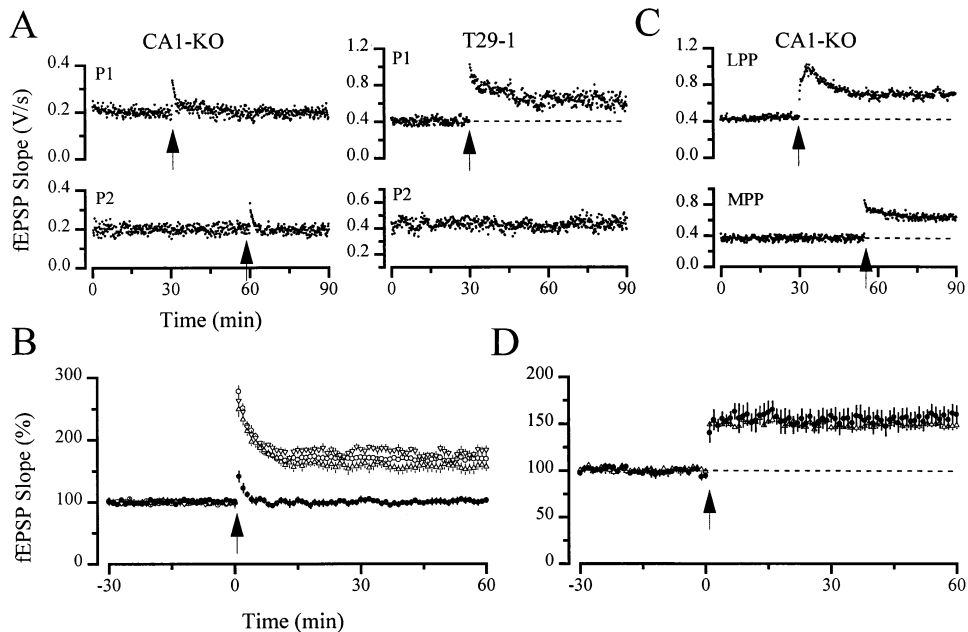


Figure 6. Lack of LTP in CA1 and Normal LTP in Dentate Gyrus from CA1-KO Mice

(A) Representative experiments in a CA1-KO slice (left) and a T29-1 slice (right). Field EPSPs were recorded in the stratum radiatum in CA1 by stimulating two independent inputs (labeled P1 and P2). After a period of baseline recording (30 min), a tetanic train (100 Hz for 1 s) was given to P1 (arrow). This pathway remained unchanged in the CA1-KO slice, whereas it became potentiated in the T29-1 slice. Picrotoxin (100 μ M) was present throughout the experiments.

(B) The mean (\pm SEM) field EPSPs in the four groups tested for LTP induction in CA1. The CA1-KO (closed circles, $n = 21$) did not show LTP, whereas the other groups presented clear LTP (T29-1, open circles, $n = 12$; fNR1, upward triangles, $n = 4$; wt, downward triangles, $n = 5$).

(C) A single experiment in which dentate field EPSPs were recorded upon stimulation of two pathways, the lateral perforant path (LPP) and the medial perforant path (MPP). A tetanus (40 shocks at 100 Hz, arrow) induced clear LTP in both pathways. Picrotoxin (100 μ M) was present throughout the experiment.

(D) The mean (\pm SEM) field EPSPs in the CA1-KO (closed circles, $n = 10$) and fNR1 (open triangles, $n = 6$) dentate gyrus. Significant LTP was elicited in both groups after the tetanus.

required to find a slightly submerged platform whose location is marked by a large proximal cue, known as the "landmark" (see Experimental Procedures). We found that the mutant mice learned the task at a somewhat a slower rate but reached the same level of optimal performance as the control mice (Figure 7B). Finally, we examined the mutant and the control mice on open-field exploratory behaviors while place-related firing of hippocampal cells was monitored with multielectrode array recordings. The results from this study are presented in an accompanying article (McHugh et al., 1996 [this issue of *Cell*]).

In conclusion, our behavioral analysis reveals that the CA1-KO mice display a selective and significant deficit in spatial memory because they are unable to develop a navigational strategy in the Morris water maze. By contrast, they could perform nonspatial learning tasks that rely on simple association strategies.

Discussion

CA1 LTP Underlies the Formation of Spatial Memory

We have generated a knockout mouse strain lacking the NMDAR1 subunit in the CA1 region of the hippocampus. These mice seem to grow normally and do not present obvious behavioral abnormalities. We have shown that the mutant mice lack NMDAR-mediated EPSCs and LTP

in the CA1 region and are impaired in the hidden-platform version of the Morris water maze (a measure of spatial memory) but not in nonspatial learning tasks. Previously, it has been suggested that NMDA receptor-dependent LTP underlies the acquisition of new memories in the hippocampus (reviewed by Bliss and Collingridge, 1993; Morris et al., 1991). Our results provide a strong support for this view and makes it more specific: the NMDA receptor-dependent LTP in the CA1 region is crucially involved in the formation of certain types of memory. We cannot exclude the possibility that the NMDA receptor-dependent synaptic plasticity crucial for memory formation is LTD, given that the CA1-KO mice seem to lack NMDAR-dependent LTD. However, we think that this is unlikely because spatial learning is apparently intact in knockout mice deficient in protein kinase A that lack CA1 LTD (Brandon et al., 1995).

Comparison with Previous Evidence

Previous work has used pharmacological and genetic tools to examine whether synaptic plasticity is the mechanism for memory formation. Although the evidence is consistent with this notion many issues have remained unresolved. For example, the most sophisticated pharmacological studies that have been done thus far are based on the infusion of NMDAR antagonists directly into the brain (Morris et al., 1986; Cain et al., 1996). Since

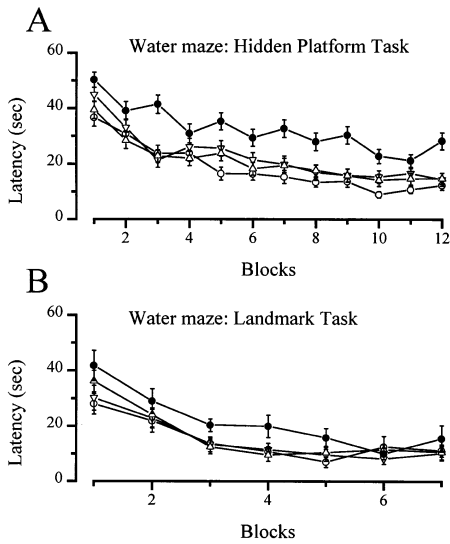


Figure 7. The Performance of CA1-KO Mice in the Water Maze
 (A) CA1-KO mice are slower in learning the hidden-platform version of the Morris water maze. The graph represents the escape latencies of mice trained to find a hidden platform in a water maze by using the distal cues surrounding it. The CA1-KO mice (closed circles, $n = 11$) display a longer latency in every block (four trials per day) than the control mice (T29-1, open circles, $n = 12$; fNR1, upward triangles, $n = 13$; wt, downward triangles, $n = 12$). Also, CA1-KO mice do not reach the optimal performance attained by the control mice, even though the mutants show some improvement.
 (B) CA1-KO mice appear normal in the performance of the landmark task in the water maze. The graph represents the escape latencies of mice trained to find a hidden platform in a water maze by using the proximal cue (a black rectangle attached to the pool wall). The CA1-KO mice (closed circles, $n = 6$) display a somewhat longer latency during the initial block (three trials per day) but improved their performance to the same level than the control mice (T29-1, open circles, $n = 6$; fNR1, upward triangles, $n = 6$; wt, downward triangles, $n = 6$).

the infusion cannot be localized to a particular region (such as the CA1 region) with the exclusion of the rest of brain, it is not possible to determine the contribution of specific areas to memory formation. Moreover, it has been reported that NMDARs contribute substantially to the basal synaptic transmission in some areas of the neocortex (Hestrin, 1996). Thus, the memory impairment could be explained at least in part by a defect in the computational ability of the neocortex rather than by an impairment in the synaptic plasticity within the hippocampus.

Several drawbacks also accompany the conventional gene knockout studies. In particular, the ubiquitous deletion of the gene may cause undesirable developmental and behavioral consequences. Our work circumvents these concerns because the deletion of the NMDAR1 subunit occurs in a restricted manner, only in the CA1 region. We have not yet shown directly the precise developmental timing of the *Cre/loxP* recombination that deletes the *NMDAR1* gene. However, an accompanying article (Tsien et al., 1996) in which we use the expression of β -galactosidase as a reporter for the recombination shows that it occurs during the third postnatal week, about 2 weeks after the CA1 region of the hippocampus has completed its cellular organization and connections

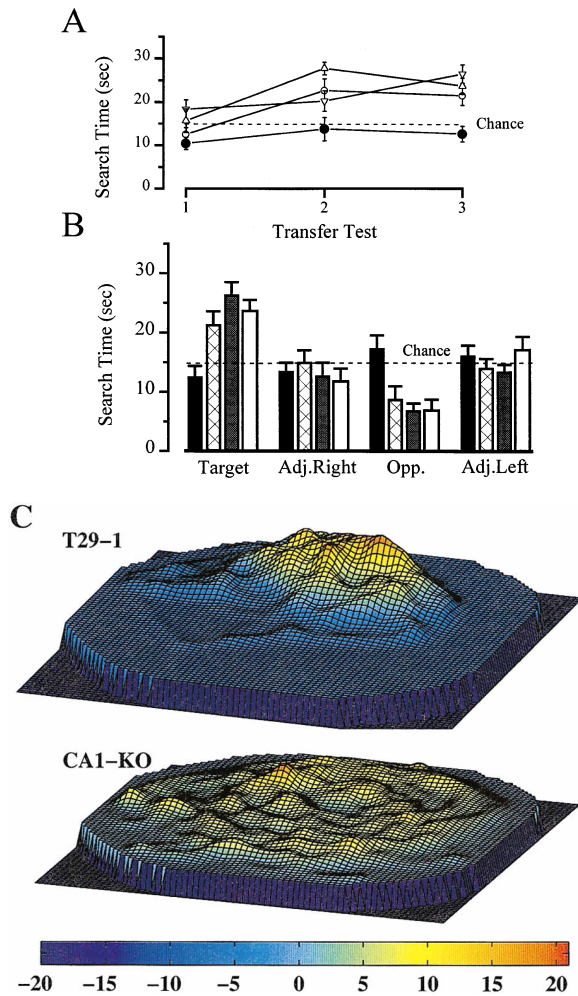


Figure 8. CA1-KO Mice Show a Deficient Performance during the Transfer Test

(A) Comparison of the average time in the target quadrant (\pm SEM) in transfer tests (TTs) 1, 2, and 3 by the four groups of mice. All groups performed at chance level (15 s) in TT1. The mutants (closed circles, $n = 11$) did not improve their performance in the subsequent TTs. The three control groups (T29-1, open circles, $n = 12$; fNR1, upward triangles, $n = 13$; wt, downward triangles, $n = 12$) spent significantly more time than chance in the target quadrant during TT2 and TT3.
 (B) Average time (\pm SEM) in each quadrant during TT3 for the four groups (closed bars, CA1-KO; hatched bars, T29-1; shaded bars, fNR1; open bars, wt). The CA1-KO mice spent equal amounts of time in every quadrant, whereas the control groups spent significantly more time than chance in the target quadrant.
 (C) Three-dimensional graphs representing the total occupancy by six T29-1 mice and six CA1-KO mice during the last transfer test. The control mice focused their search in the trained location (where the platform used to be during training) whereas the mutant mice visited the whole maze area equivalently.

(Pokorny and Yamamoto, 1981a, 1981b; Stanfield and Cowan 1979). Thus, it is likely that the *NMDAR1* gene is also deleted at this time, providing a postnatal knockout of the gene and thus avoiding the developmental concerns.

Consideration into the Mixed Genetic Background
 Another caveat associated with the behavioral studies done in gene knockout mice stems from the fact that

ES cells from the mouse strain 129/Sv are commonly used to generate the mutant mice (reviewed by Gerlai, 1996). The 129/Sv mice demonstrate behavioral defects such as the inability to perform the Morris water maze task (Gerlai, 1996). Consequently, most behavioral studies with knockout mice have been carried out after crossing them to a behaviorally “normal” strain, such as C57BL/6. This of course causes animal-to-animal variations in the ability to perform a certain behavioral task, variation that is attributed to the difference in the genetic background. The problem is best resolved by using ES cells derived from a behaviorally normal strain, such as C57BL/6. Recently, ES cells from this strain that have an acceptable frequency of germline transmission have become available (Kawase et al., 1994; Köntgen et al., 1993; Ledermann and Bürki, 1991). In the current study, the genetic background issue has not been resolved completely. However, we avoided a major source of variation for the Morris water maze task by eliminating “floating” individuals from both the mutant and control groups (see Experimental Procedures).

Gene Knockout Studies Point to a Pivotal Role of CA1 Synaptic Plasticity

Previous studies examined the correlation between spatial memory and the site of hippocampal LTP (i.e., CA1, CA3, and dentate gyrus) by using a variety of conventional knockout mice (reviewed by Chen and Tonegawa, 1997). These studies found a correlated impairment in ScC-CA1 LTP and spatial memory (but see Conquet et al., 1994). It is important to point out that the only exceptional case, namely that of the mGluR1 mutant mice, is complicated by the fact that two groups have generated and analyzed these mutants independently and have obtained opposing results (Aiba et al., 1994; Conquet et al., 1994; Chen and Tonegawa, 1997). By contrast, it has been shown that impairments of mossy fiber-CA3 LTP (Huang et al., 1995) and perforant path-dentate LTP (Nosten-Bertrand et al., 1996) are not correlated with spatial memory deficit.

Our new evidence, while still correlational, is much stronger than that in the earlier reports because we have singled out the CA1 synapses as a site of plasticity impairment. What structural and functional features could explain this pivotal role of CA1 synapses as sites of plasticity underlying spatial memory? It is well known that the CA1 region is a crucial component of the “hippocampal formation” system that is involved in the acquisition of certain types of memory. In rodents, this system consists of several structures connected within a loop that encompasses (Figure 9) the entorhinal cortex (EC), with inputs from higher sensory cortices; dentate gyrus (DG), with inputs from EC; CA3, with “external” inputs from EC and DG and “internal” inputs from CA3; CA1, with inputs from CA3 and EC; and subiculum (SUB), with inputs from CA1 and outputs to EC (Lorente de Nó, 1934; Amaral and Witter, 1989). In lieu of the evidence currently available, it would seem that the minimal system required as a locus for memory acquisition would be the EC-CA3-CA1-SUB-EC loop. This is because first, the plasticity in the EC-DG and DG-CA3 synapses seems to be dispensable (Huang et al., 1995; Nosten-Bertrand et al., 1996); second, the direct EC-CA1 connection appears to be too weak to sustain the EC-CA1-SUB-EC

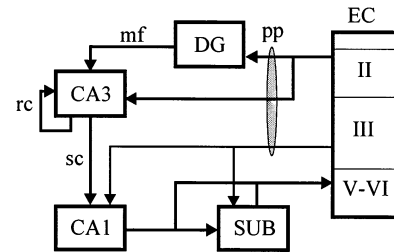


Figure 9. Connections in the Hippocampal Memory System

The excitatory pathways in the hippocampal formation. EC, entorhinal cortex; DG, dentate gyrus; mf, mossy fibers; pp, perforant path; rc, recurrent collateral axons of the CA3 pyramidal neurons; sc, Schaffer collateral/commissural axons; SUB, subiculum.

loop as the locus for memory (Empson and Heinemann, 1995); and third, the evidence presented in this article points to the special role of the CA3-CA1 synapses.

The plasticity of the EC-CA3 synapses has not been well studied, but our proposed scenario predicts that they are important in implementing the memory system. Most probably, both the EC-CA3 pathway and the EC-DG-CA3 pathway provide parallel inputs to the CA3 network during learning, and the CA3-CA3 synapses work as autoassociative memory devices, as has long been proposed (Marr, 1971). Thus, it is desirable to generate a CA3 region-specific knockout of the NMDA receptor to allow direct examination of the contribution of these synapses to learning.

Experimental Procedures

Targeting Vector and Generation of NMDAR1 Mutant Mice

A mouse 129/SvJ cosmid library (Stratagene) was screened with a probe corresponding to the mouse *NMDAR1* gene exon 19. A clone covering the first intron, transmembrane domain, and C-terminal region of the *NMDAR1* gene as well as its 3' downstream region (total ~45 kb) was isolated and mapped by restriction digestion. The replacement-type targeting vector (Figure 1A) was made by inserting the first *loxP* site into a 5 kb intron between exons 10 and 11. The second *loxP* site along with the *pgk-neo* gene was inserted into an *Xba* site 3 kb downstream of the last exon with the same orientation as that of the first *loxP* site. The two *loxP* sites flanked an ~12 kb genomic region spanning the entire transmembrane domain and C-terminal region. The targeting vector contained 16 kb of homologous DNA upstream (left arm) of the first *loxP* site and 6 kb of homologous DNA downstream (right arm) of the second *loxP* site/*pgk-neo* gene.

The linearized targeting vector was electroporated into J1 cells derived from 129/terSv (Li et al., 1994) maintained on subconfluent embryonic fibroblasts. Neomycin-resistant ES cell colonies were picked and expanded. The ES cells harboring homologous recombination were determined by Southern blotting using a 5' probe and a 3' probe, which correspond to the gene regions depicted in Figure 1A. The targeted ES cells were injected into C57BL/6 blastocysts. These blastocysts were transferred into pseudopregnant mothers. Chimeric mice with more than 90% agouti were bred against C57BL/6. The F1 mice with germline transmission of the *fNR1* gene were bred with the transgenic line T29-1. The F2 offspring heterozygous for both the *fNR1* gene and the *Cre* transgene (*Cre*+, *fNR1*+) were mated with heterozygous *fNR1* mice (+/+, *fNR1*+/+) to obtain F3 mice carrying the *Cre* transgene as well as the homozygous *fNR1* gene (*Cre*+, *fNR1*/*fNR1*), that is, CA1-KO mice. The genotype distribution among the total F3 progeny (from the second mating) was 23:21:46:42:22:23 for wt (+/+, +/+), T29-1 transgenic (*Cre*+, +/+), heterozygous *Cre* and *fNR1* (*Cre*+, *fNR1*/+), heterozygous *fNR1* (+/+, *fNR1*/+), homozygous *fNR1* (+/+, *fNR1*/*fNR1*), and CA1-KO (*Cre*+, *fNR1*/*fNR1*), respectively. This distribution is close to

the 1:1:2:2:1:1 Mendelian ratio expected for the segregation of two independent loci (with no embryonic lethality).

Southern Blot and Polymerase Chain Reaction Analysis

Purified DNA from mouse tails was digested with the indicated restriction enzymes (EcoRI or EcoRV), fractionated by electrophoresis through 0.7% agarose gels, transferred onto Zeta-probe GT membranes (BioRad), and hybridized with a 5' probe (exons 7 and 8) or a 3' probe (1.2Xba fragment), or both, for the *NMDAR1* gene (Figure 1A). The *Cre* transgene was typed by polymerase chain reaction using 5' and 3' primers, as described in the accompanying article (Tsien et al., 1996).

Histology and In Situ Hybridization

The mouse brains were perfused with iced-cold phosphate-buffered saline (PBS) buffer and 30% sucrose, dissected, and rapidly frozen in the mounting medium. Cryostat sections (20 μ m) were prepared and postfixed for 5 min in 4% paraformaldehyde in PBS buffer (pH 7.5). After washing twice in PBS (5 min each wash), the slices were stained with cresyl violet. Light microscopy was performed from 1.25 \times to 20 \times magnification on a Nikon microscope.

For in situ hybridization, the slices were hybridized to a 45-mer probe (sequence 5'-CTCCTCCTCTCGCTGTTACACCTTAAATCGGCCAAAGGGACT-3'). This corresponds to the region between the first and the second transmembrane domains, which is located within a sequence flanked by the two *loxP* sites. Upon *Cre*-mediated recombination, this region is expected to be deleted at the DNA level. The probes were labeled by 3'-poly(A) tailing using nonradioactive fluorescein-11-dUTP and terminal transferase. Hybridization solution was supplied by the manufacturer (Amersham) with addition of 3'-poly(A) (100 μ g/ml) and of denaturated salmon sperm DNA (100 μ g/ml). Slides were washed for 5 min at room temperature and 1 \times SSC, 0.01% SDS for 1 min, and 0.1 \times SSC at 37°C for 10 min. For cytochrome oxidase histochemistry, the brains were perfused with cold saline and 4% paraformaldehyde in PBS buffer (0.1 M), dissected, and submerged in 30% sucrose for 2 days at 4°C before sectioning with a Vibratome. Cytochrome oxidase staining was performed using the protocol described by Wong-Riley (1979).

Electrophysiology

Mice (21–48 days old) were anesthetized with metaflurane and sacrificed by decapitation. The brain was quickly removed and submerged in artificial cerebrospinal fluid (ACSF) solution at \sim 4°C for \sim 3 min. The ACSF contained (in mM): 124 NaCl, 26 NaH₂CO₃, 10 D-glucose, 5 KCl, 2 CaCl₂, 2 MgSO₄, and 1.2 NaH₂PO₄ (pH 7.2) and was oxygenated with a 95% O₂-5% CO₂ gas mixture. The brain was further sectioned into a block (which included the hippocampus) and glued to the stage of a Vibratome. Transverse hippocampal slices (350 μ m thick) were cut and transferred to a holding chamber and kept at 37°C for the first \sim 45 min and at room temperature for the rest of the experiment. Recordings were made 2–6 hr after dissection. A single hippocampal slice was transferred to a submerged recording chamber and a cut was made between the CA3 and CA1 regions. The slice was bathed with rapidly flowing (1 ml/min) oxygenated ACSF containing picrotoxin (100 μ M). Bath temperature was maintained at 30–32°C with a heating controller unit (TC-324, Warner). The recording chamber was mounted on upright fixed-stage microscope (Zeiss).

Intracellular patch-clamp recordings, in the whole-cell mode, were made (reviewed by Sakmann and Stuart, 1995). Infrared illumination coupled to DIC optics with a 40 \times water immersion objective (Zeiss) enabled us to visualize the cell bodies of CA1 pyramidal neurons in the superficial layer of the slice, allowing assessment of the health of the slice and recordings of identified neurons under visual guidance (Edwards et al., 1989; Sakmann and Stuart, 1995). Patch electrodes (resistance, 5–7 M Ω) were pulled from thin-walled glass pipettes (150F-4, WPI) and filled with internal solution containing (in mM): 140 K-gluconate, 1.1 EGTA, 0.1 CaCl₂, 10 HEPES, 2 Mg-ATP, 1 MgCl₂, and 0.3 Na-GTP (pH 7.2). Access resistances were measured regularly during recording (typical values were 10–20 M Ω). Synaptic responses were evoked by stimulating with a bipolar Pt/Ir electrode placed in stratum radiatum (\sim 50–400 μ m to the side of the recorded cell and 50–100 μ m from stratum pyramidale). Stimuli (50 μ s, 0.1–0.7

mA) produced EPSCs, which were amplified with an Axopatch 1D amplifier (Axon Instruments), digitized with an analog-to-digital board (Digidata 1200A, Axon), and analyzed on-line by adsllice data-collection software (written by P. Huerta). The NMDA currents were isolated pharmacologically by adding the following to the ACSF: CNQX (20 μ M), picrotoxin (100 μ M), 2-OH-saclofen (200 μ M), and glycine (1 μ M) and by removing Mg²⁺ from the ACSF.

Extracellular recordings of field EPSPs were made with glass pipettes filled with 2 M NaCl (resistance, 1–2 M Ω). To obtain CA1 EPSPs, the recording electrode was positioned in stratum radiatum (50–100 μ m from stratum pyramidale), and two stimulating electrodes were placed in stratum radiatum, at either side of the recording electrode, for alternative stimulation of two independent inputs. The lack of cross-facilitation between the inputs was used a criterion for independence. Stimulation intensity was adjusted for responses that were 50% of the maximal EPSP. For dentate gyrus recordings, the recording electrode was positioned in stratum moleculare (300 μ m from stratum granulosum), and two stimulating electrodes were located at opposite sides for stimulating perforant path inputs alternatively. The evoked EPSPs were amplified (AM Systems 1700), digitized (2 kHz sampling rate), and analyzed on-line by adsllice software. For tetanic stimulation, the stimulation intensity was increased to twice the test stimulation. The standard tetanus was a train of 100 Hz for 1 s. Statistical differences between the tetanized pathway and the control pathway were tested on 30 responses from each pathway (45 min after tetanus) by Student's *t* test (Huerta and Lisman, 1995).

Behavioral Testing

We used two standard water maze tasks to test for spatial and nonspatial memory (Morris et al., 1982; Kolb et al., 1994). To measure spatial memory, we used the hidden-platform task in four groups of mice: CA1-KO (*n* = 11), fNR1 (*n* = 13), T29-1 (*n* = 12), and wt (*n* = 12) mice. The apparatus consisted of a circular pool (white plastic, 120 cm diameter, 79 cm height) containing water (80 cm high) at 21–22°C, which was made opaque white by adding tempera. The pool was surrounded by a black curtain (90 cm from the periphery of the pool). Three rectangular drawings (50 \times 70 cm²) with geometric designs, placed on the curtain wall (120 cm height) and brightly illuminated, served as the distal cues. The mice did not swim in the pool before training (i.e., there was no habituation) but were simply placed on the platform for \sim 30 s. Mice that initiated swimming spontaneously were not returned to the platform. During the training sessions, mice that did not show motivation for swimming (i.e., “floaters”) in any of the trials were excluded from the task and replaced by siblings. Overall, the floating behavior was more prominent in the fNR1 mice (\sim 20% of the tested animals) than in the other mice. The mice were trained to find the hidden platform (circle of 12 cm in diameter, submerged 1 cm below the water level) by swimming 4 trials every day. Within each group, half of the mice were trained with the platform in the southwest quadrant and the others in the northeast quadrant. If a mouse did not find the platform in 1 min, it was stopped and placed over the platform for \sim 10 s. The mice were tracked by an infrared-sensitive camera connected to a tracker unit (Dragon). The tracked positions were stored on videotape and collected by ad software (written by M. Wilson and L. Frank, Massachusetts Institute of Technology). A transfer test was given at the end of days 1, 6, and 12. For this test, the mouse swam for 60 s in the absence of the platform. Analysis of the swimming paths was performed by mazeextract software (written by M. Wilson).

To measure nonspatial learning we used the landmark task, as described by Kolb et al. (1994). The same water maze was used as in the hidden-platform task with one difference to the procedure: the platform was moved on each block of trials and its location was marked by a landmark consisting of a 20 \times 12 cm² black rectangle mounted on the pool wall \sim 25 cm away from the platform. There were three trials every day.

Acknowledgments

We would like to thank Jason Derwin, Tamara Ochoa, and Cindy Tom for their assistance; Kenneth I. Blum and Takuji Iwasato for

comments on the manuscript, Athanassios Siapas for help with Figure 8C; and Matthew Wilson for insightful discussion and guidance throughout this project. This work was supported by National Institutes of Health grant number NS32925 and by gifts from Shionogi Institute for Medical Science and Amgen, Inc. (all to S. T.). P. T. H. was also supported by the Pew Latin American Fellows Program.

Received November 8, 1996; revised November 25, 1996.

References

- Aiba, A., Chen, C., Herrup, K., Rosenmund, C., Stevens, C.F., and Tonegawa, S. (1994). Reduced hippocampal long-term potentiation and context-specific deficit in associative learning in mGluR1 mutant mice. *Cell* 79, 365–375.
- Amaral, D., and Witter, M. (1989). The three-dimensional organization of the hippocampal formation: a review of anatomical data. *Neuroscience* 31, 571–591.
- Bannerman, D., Good, M., Butcher, S., Ramsay, M., and Morris, R.G.M. (1995). Distinct components of spatial learning revealed by prior training and NMDA receptor blockade. *Nature* 378, 182–186.
- Bliss, T.V.P., Collingridge, G.L. (1993). A synaptic model of memory: long-term potentiation in the hippocampus. *Nature* 361, 31–39.
- Bliss, T.V.P., and Lomo, T. (1973). Long-lasting potentiation of synaptic transmission in the dentate area of the anaesthetized rabbit following stimulation of the perforant path. *J. Physiol. Lond.* 232, 331–356.
- Bradley, A. (1987). Production and analysis of chimeric mice. In *Teratocarcinomas and Embryonic Stem Cells: A Practical Approach*, E.J. Robertson, ed. (Oxford: IRL Press), pp. 113–151.
- Brandon, E.P., Zhuo, M., Huang, Y.Y., Qi, M., Gerhold, K.A., Burton, K.A., Kandel, E.R., McKnight, G.S., and Idzerda, R.L. (1995). Hippocampal long-term depression and depotentiation are defective in mice carrying a targeted disruption of the gene encoding the R1 β subunit of the cAMP-dependent protein kinase. *Proc. Natl. Acad. Sci. USA* 92, 8851–8855.
- Butcher, S.P., Hamberger, A., and Morris, R.G. M. (1991). Intracerebral distribution of DL-2-aminophosphopentanoic acid (AP5) and the dissociation of different types of learning. *Exp. Brain Res.* 83, 521–526.
- Cain, D.P., Saucier D., Hall, J., Hargreaves, E., and Boon F. (1996). Detailed behavioral analysis of water maze acquisition under APV or CNQX: contribution of sensorimotor disturbances to drug-induced acquisition deficits. *Behav. Neurosci.* 110, 86–101.
- Capecchi, M.R. (1989). Altering the genome by homologous recombination. *Science* 244, 1288–1292.
- Chen, C., and Tonegawa, S. (1997). Molecular genetic analysis of synaptic plasticity, activity-dependent neural development, learning, and memory in the mammalian brain. *Ann. Rev. Neurosci.*, in press.
- Collingridge, G.L., Kehl, S., and McLennan, H. (1983). Excitatory amino acids in synaptic transmission in the Schaffer collateral-commissural pathway of the rat hippocampus. *J. Physiol. Lond.* 334, 33–46.
- Conquet, F., Bashir, Z.I., Davies, C.H., Daniel, H., Ferraguti, F., et al. (1994). Motor deficit and impairment of synaptic plasticity in mice lacking mGluR1. *Nature* 372, 237–243.
- Dudek, S., and Bear, M. (1992). Homosynaptic long-term depression in area CA1 of hippocampus and effects of N-methyl-D-aspartate receptor blockade. *Proc. Natl. Acad. Sci. USA* 89, 4363–4367.
- Edwards, F., Konnerth, A., Sakmann, B., and Takahashi, T. (1989). A thin slice preparation for patch clamp recordings from neurones of the mammalian central nervous system. *Pflügers Arch.* 414, 600–612.
- Empson, R.M., and Heinemann, U. (1995). The perforant path projection to hippocampal area CA1 in the rat hippocampal-entorhinal cortex combined slice. *J. Physiol. Lond.* 484, 707–720.
- Forrest, D., Yuzaki, M., Soares, H.D., Ng, L., Luk, D.C., Sheng, M., Stewart, C.L., Morgan, J.I., Connor J. A., and Curran, T. (1994). Targeted disruption of NMDA receptor 1 gene abolishes NMDA response and results in neonatal death. *Neuron* 13, 325–338.
- Gerlai, R. (1996). Gene-targeting studies of mammalian behavior: is the mutation or the background genotype? *Trends Neurosci.* 19, 177–181.
- Grover, L., and Teyler, T. (1990). Two components of long-term potentiation induced by different patterns of afferent activation. *Nature* 347, 477–479.
- Hanse, E., and Gustafsson, B. (1992). Long-term potentiation and field EPSPs in the lateral and medial perforant paths in the dentate gyrus *in vitro*: a comparison. *Eur. J. Neurosci.* 4, 1191–1201.
- Hebb, D.O. (1949). *The Organization of Behavior* (New York: John Wiley).
- Hestrin, S. (1996). Physiology of NMDA receptors and synaptic currents. In *Excitatory Amino Acids and the Cerebral Cortex*, F. Conti and T.P. Hicks, eds. (Cambridge, Massachusetts: MIT Press), pp. 53–62.
- Hestrin, S., Nicoll, R., Perkel, D., and Sah, P. (1990a). Analysis of excitatory synaptic action in pyramidal cells using whole-cell recording from rat hippocampal slices. *J. Physiol. Lond.* 422, 203–225.
- Hestrin, S., Sah, P., and Nicoll, R. (1990b). Mechanisms generating the time course of dual component excitatory synaptic currents recorded in hippocampal slices. *Neuron* 5, 247–253.
- Huang, Y.-Y., Kandel, E.R., Varshavsky, L., Brandon, E.P., Qi, M., Idzerda, R.L., McKnight, G.S., and Bourchouladze, R. (1995). A genetic test of the effects of mutations in PKA on mossy fiber LTP and its relation to spatial and contextual learning. *Cell* 83, 1211–1222.
- Huerta, P.T., and Lisman, J.E. (1995). Bidirectional synaptic plasticity induced by a single burst during cholinergic theta oscillation in CA1 *in vitro*. *Neuron* 15, 1053–1063.
- Huerta, P.T., Searce, K., Farris, S., Empson, R., and Prusky, G. (1996). Preservation of spatial learning in *fyn* tyrosine kinase knockout mice. *NeuroReport* 7, 1685–1689.
- Kawase, E., Suemori, H., Takahashi, N., Okazaki, K., Hashimoto, K., and Nakatsuji, N. (1994). Strain difference in the establishment of mouse embryonic stem (ES) cell lines. *Int. J. Dev. Biol.* 38, 385–390.
- Kolb, B., Buhmann, K., McDonald, R., and Sutherland, R. (1994). Dissociation of the medial prefrontal, posterior parietal, and posterior temporal cortex for spatial navigation and recognition memory in the rat. *Cerebral Cortex* 4, 664–680.
- Köntgen, F., Suss, G., Steward, C., Steinmetz, M., and Bluethmann, H. (1993). Targeted disruption of the MHC class II Aa gene in C57BL/6 mice. *Int. Immunol.* 5, 957–964.
- Ledermann, B., and Bürki, K. (1991). Establishment of a germ-line competent C57BL/6 embryonic stem cell line. *Exp. Cell Res.* 197, 254–258.
- Li, Y., Erzurumlu, R., Chen, C., Jhaveri, S., and Tonegawa, S. (1994). Whisker-related neuronal patterns fail to develop in the trigeminal brainstem nuclei of NMDAR1 knockout mice. *Cell* 76, 427–437.
- Lorente de Nó, R. (1934). Studies of the structure of the cerebral cortex. II: Continuation of the study of the ammonic system. *J. Psychol. Neurol.* 46, 113–177.
- Marr, D. (1971). Simple memory: a theory for archicortex. *Philos. Trans. R. Soc. Lond. B Biol. Sci.* 262, 23–81.
- McBain, C., and Mayer, M. (1994). N-methyl-D-aspartic acid receptor structure and function. *Physiol. Rev.* 74, 723–760.
- McHugh, T.J., Blum, K.I., Tsien, J.Z., Tonegawa, S., and Wilson, M.A. (1996). Impaired hippocampal representation of space in CA1-specific NMDAR1 knockout mice. *Cell* 87, this issue.
- Moriyoshi, K., Masu, M., Ishii, T., Shigemoto, R., Mizuno, N., Nakanishi, S. (1991). Molecular cloning and characterization of the rat NMDA receptor. *Nature* 354, 31–37.
- Morris, R.G.M., Garrud, P., Rowlins, J.N.P., and O'Keefe, J. (1982). Place navigation impaired in rats with hippocampal lesions. *Nature* 297, 681–683.

- Morris, R.G.M., Anderson, E., Lynch, G., and Baudry M. (1986). Selective impairment of learning and blockade of long-term potentiation by an *N*-methyl-D-aspartate receptor antagonist, AP5. *Nature* 319, 774–776.
- Morris, R.G.M., Davis, S., and Butcher, S.P. (1991). Hippocampal synaptic plasticity and NMDA receptors: a role in information storage? In *Long-Term Potentiation: A Debate of Current Issues*, M. Baudry and J. Davis, eds. (Cambridge, Massachusetts: MIT Press), pp. 267–300.
- Nakanishi, S. (1992). Molecular diversity of glutamate receptors and implications for brain function. *Science* 258, 597–603.
- Nosten-Bertrand, M., Errington, M., Murphy, K., Tokugawa, Y., Barboni, E., Kozlova, E., Michalovich, D., Morris, R.G. M., Silver, J., Stewart, C., et al. (1996). Normal spatial learning despite regional inhibition of LTP in mice lacking Thy-1. *Nature* 379, 826–829.
- Nowak, L., Bregestovski, P., Ascher, P., Herbert, A., Prochiantz, A. (1984). Magnesium gates glutamate-activated channels in mouse central neurones. *Nature* 307, 462–465.
- Pokorny, J., and Yamamoto, T. (1981a). Postnatal ontogenesis of hippocampal CA1 area in rats. I. Development of dendritic arborisation in pyramidal neurons. *Brain Res. Bull.* 7, 113–120.
- Pokorny, J., and Yamamoto, T. (1981b). Postnatal ontogenesis of hippocampal CA1 area in rats. II. Development of ultrastructure in stratum lacunosum and moleculare. *Brain Res. Bull.* 7, 121–130.
- Rawlins, J.N.P. (1996). NMDA receptors, synaptic plasticity, and learning and memory. In *Excitatory Amino Acids and the Cerebral Cortex*, F. Conti and T.P. Hicks, eds. (Cambridge, Massachusetts: MIT Press), pp. 275–284.
- Sakmann, B., and Stuart, G. (1995). Patch-pipette recordings from the soma, dendrites, and axons of neurons in brain slices. In *Single-Channel Recording*, 2nd ed., B. Sakmann and E. Neher, eds. (New York: Plenum Press), pp. 199–211.
- Scoville, W.B., and Milner, B. (1957). Loss of recent memory after bilateral hippocampal lesions. *J. Neurol. Neurosurg. Psychiatry* 20, 11–12.
- Silva, A., Stevens, C.F., Tonegawa, S., and Wang, Y. (1992a). Deficient hippocampal long-term potentiation in α -calcium calmodulin kinase II mutant mice. *Science* 257, 201–206.
- Silva, A., Paylor, R., Wehner, J., and Tonegawa, S. (1992b). Impaired spatial learning in α -calcium calmodulin kinase II mutant mice. *Science* 257, 206–211.
- Squire, L.R. (1987). *Memory and Brain*. (New York: Oxford University Press).
- Stanfield, B.B., and Cowan, W. (1979). The development of the hippocampus and dentate gyrus in normal and reeler mice. *J. Comp. Neurol.* 185, 423–459.
- Tsien, J.Z., Chen, D.F., Gerber, D., Tom, C., Mercer, E., Anderson, D. J., Mayford, M., Kandel E. R., and Tonegawa, S. (1996). Subregion- and cell type-restricted gene knockout in mouse brain. *Cell* 87, this issue.
- Wong-Riley, M. (1979). Changes in the visual system of monocularly sutured or enucleated cats demonstrable with cytochrome oxidase histochemistry. *Brain Res.* 171, 11–28.
- Zalutsky, R., and Nicoll, R. (1990). Comparison of two forms of long-term potentiation in single hippocampal neurons. *Science* 248, 1619–1624.
- Zola-Morgan, S., Squire, L.R, and Amaral, D. (1986). Human amnesia and the medial temporal region: enduring memory impairment following a bilateral lesion limited to field CA1 of the hippocampus. *J. Neurosci.* 6, 2950–2967.